

KINETIC STUDY OF THE UO_2/C INTERACTION BY HIGH TEMPERATURE MASS SPECTROMETRY

S. Gossé

CEA Saclay – DEN/DANS/DPC/SCP/LM2T
91191 Gif-sur-Yvette Cedex, France

S. Chatain

CEA Saclay – DEN/DANS/DPC/SCP/LM2T
91191 Gif-sur-Yvette Cedex, France

C. Chatillon

LTPCM – CNRS, ENSEEG BP75 Grenoble
38402 Saint-Martin d'Hères Cedex, France

C. Guéneau

CEA Saclay – DEN/DANS/DPC/SCP/LM2T
91191 Gif-sur-Yvette Cedex, France

B. Larousse

CEA Saclay – DEN/DANS/DPC/SCP/LM2T
91191 Gif-sur-Yvette Cedex, France

F. Le Guyadec

CEA Pierrelatte – VRH/DTEC/STCF/LMAC
BP 111 – 26700 Pierrelatte, France

ABSTRACT

For Very High Temperature Reactors (VHTR), one of Generation IV future systems, the high level operating temperature of the fuel materials in normal and accidental conditions requires to predict the possible chemical interactions between the fuel component (UO_2) and the structural materials (C, SiC). Among the concerns of the TRISO particle thermo-mechanical behaviour, it is necessary to better understand the gaseous carbon oxides formation at the fuel-buffer interface that leads to the build up of the internal pressure. High equilibrium $CO_{(g)}$ pressures resulting of the UO_{2+x}/C reaction are obtained using thermodynamic calculations. The kinetic mechanisms involved in this reaction that limit this pressure increase have to be determined by convenient experiments and associated models. Some of the reported data on the kinetic of $CO_{(g)}$ formation due to the UO_{2+x} and graphite interaction have been reviewed. The discrepancies between the reaction mechanisms can be explained (i) by the different geometries and sample types and (ii) by the oxide stoichiometry and the flowing gas used during the experiments. Depending on these characteristics, the phenomena involved in $CO_{(g)}$ formation can be of three different kinds : Interface, Surface or Diffusion. Using High Temperature Mass Spectrometry (HTMS), kinetic measurements of the $CO_{(g)}$ and $CO_{2(g)}$ species due to the interaction between UO_{2+x} and graphite were performed. The samples are pressed pellets constituted of a mixture of UO_{2+x} and graphite powders with molar compositions $C/UO_{2+x} = 3/5$. CO (g) is the major product above 1200 K. Rates of the $CO_{(g)}$ formation have been established taking into account the oxygen composition of the non-stoichiometric uranium dioxide and temperature. Results underline the utmost importance of kinetic factors for studying the $CO_{(g)}$ pressure variation inside the TRISO particle.

INTRODUCTION

The TRISO particle is one of the retained fuels for the generation IV Very High Temperature Reactors (VHTR). This study deals with the chemical interaction between the UO_{2+x} fuel kernel and its surrounding graphite matrix which has to accommodate noble fission products and CO and CO_2 gas releases. A previous work was undertaken on the thermodynamic properties of the Uranium-Carbon-Oxygen ternary system [1] and on the $CO_{(g)}$ associated equilibrium pressures [2]. In fact, it is important to establish the maximum CO and CO_2 gas pressures produced inside the fuel particle due to the interaction between the UO_{2+x} kernel and the graphite buffer (Figure 1). When estimated by using thermodynamic calculations, the pressure values are largely higher than those observed.

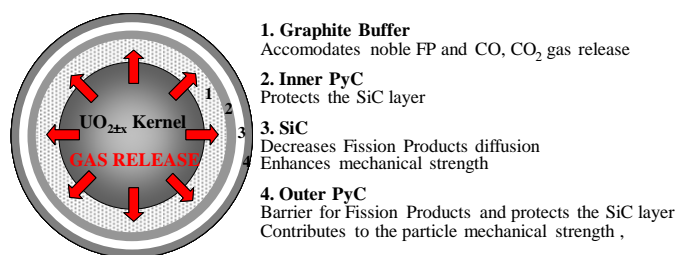


Figure 1: TRISO Particle for High Temperature Reactor

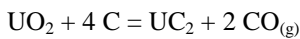
Thus, it is also necessary to determine the formation rates of CO and CO_2 (g) which will be used as input data for calculation codes that model the thermo-mechanical behaviour of the VHTR fuel particles. A thorough study of the high temperature behaviour of a mixture of UO_2 and carbon is then necessary in order to establish the kinetics of the interaction between both materials. The objectives are (i) to predict the possible formation of carbide phases and (ii) to

establish the controlling mechanisms of the UO_{2+x}/C interaction kinetics.

The origin of this interaction can be explained by phenomena of surface, diffusion or interface. The first part of the present work consists in reviewing several kinetic models of the literature. Initially, the experimental methods used to establish the kinetics of interaction are described. Then, the second part deals with the experimental results obtained by High Temperature Mass Spectrometry (HTMS). These first kinetic results, coupled to metallographic analyses of the samples make it possible to validate some assumptions on the reactional mechanisms.

KINETIC OF INTERACTION

Several studies relate to the kinetics of interaction between UO_2 and carbon and this, for several reasons. First, these compounds are the two reagents of the carbothermic reaction, which remains an important synthesis route of uranium carbide. It is thus to increase the reaction yield and to favour selective syntheses of the uranium dicarbide that the following reaction was specifically studied.



However, these studies were mainly carried out with the aim of establishing the kinetics of formation of carbide and not that of $\text{CO}_{(\text{g})}$ and/or $\text{CO}_{2(\text{g})}$. They consider that the $\text{CO}_{(\text{g})}$ formation is inevitably associated with that of an uranium carbide, which is equal with being placed in a monovariant equilibrium inside the U-C-O ternary system.

The interest involved in this reaction also comes from the fact that interaction between UO_2 and the graphite buffer could lead to a carbide formation in TRISO fuels.

This reaction being reversible, various projects plan to introduce a mixture of UO_2 and UC_2 as a fuel, in order to maintain a low start value of $\text{CO}_{(\text{g})}$ pressure inside the particle which tends to increase with the irradiation [3]. However, in the case of an UO_2 fuel (what thus excluded the $\text{UO}_2 + \text{UC}_2$ mixtures), the equilibrium is not monovariant but bivariant. $\text{CO}_{(\text{g})}$ pressures are then not only a function of the temperature but also of the chemical composition of the system.

These kinetics are difficult to establish on the one hand because they are solid-solid and heterogeneous solid-gas reactions and on the other hand, because many parameters must be considered in this study. The relative quantities of the reagents as well as the geometry and the particle sizing of the components have a paramount importance on measured reactional rates.

Several models deal with interaction kinetics between two solid phases. They can be used in the case of spherical symmetry of the reagents and the products. Among them, certain models consider that kinetics are limited by diffusion phenomena (Valensi-Carter, Ginstling), as that was shown in the case of the UO_2/C interaction [4] [6].

Review of the literature

The main product of the reaction between UO_2 and carbon, leading to uranium carbides production is $\text{CO}_{(\text{g})}$. Then, it is possible to follow the evolution of this system and the kinetics of the $\text{UO}_2 + \text{C}$ interaction by measurement of the mass loss of the sample by ThermoGravimetric Analysis (TGA).

According to Danger & al. [4], the reaction begins to be significant at 1773 K. Even if some discrepancies can appear on the rates, the reaction products are identical, and made of uranium monocarbide (UC) flakes inside of a uranium dicarbide (UC_2) matrix. The Valensi-Carter [5] model for powder reactions was used to describe this reaction between UO_2 spherical particles and powdered graphite. In the case of a parabolic shape of the reaction curve, and when the expansion coefficient between the reactant and the product is close to unity, it is possible to establish the kinetic law from the degree of conversion (ξ). Using the Valensi-Carter transform $F(\xi)$, the following linear function of time is obtained (Eq. 1):

$$F(\xi) = 1 - \frac{2}{3} \xi - (1 - \xi)^{\frac{2}{3}} = Kt \quad (\text{Eq. 1})$$

$$\text{Where } \xi = \frac{m_0 - m_t}{m_0 - m_f} \quad (\text{Eq. 2})$$

This rate constant (K) is the product of two components; the first one is function of the diffusion processes and of the interfacial equilibrium constants, the second one is a function of the experimental conditions [4].

In the aim of establishing the rate controlling step of the interaction between UO_2 and graphite, Lindemer & al. [6] have studied the behaviour of spherical UO_2 particles coated with graphite in the 1673-1879 K temperature range. This spherical geometry has as an advantage of simulating perfectly the expected behaviour of TRISO particles. In order to highlight the involved kinetic phenomena in this interaction (interface, surface, diffusion), the degree of conversion was determined by metallographic methods and two sample configurations (particles and pellets) were produced and studied. The model used by Lindemer & al. is that of Ginstling (Eq. 3) developed for diffusion kinetics [7]. It makes it possible to assess growth kinetics of the product layer according to the temporal decrease of the UO_2 radius $r(t)$ inside the particle and knowing this radius (r_0) at t_0 :

$$\frac{1}{3} - \left(\frac{r(t)}{r_0} \right)^2 \times \left(1 - \frac{2r(t)}{3r_0} \right) = \frac{k_D t}{r_0^2} \quad (\text{Eq. 3})$$

The cases of kinetics controlled by surface or interface phenomena have also been studied by Lindemer & al. which have used all these various models previously quoted to treat the experimental data. After a series of experiments performed at constant temperature, the phenomena controlling the kinetics can be represented according to

straight lines as a function of time. This interpretation makes it possible to consolidate the assumption of a kinetic control by a diffusion phenomenon (Figure 2). Indeed, among the linear kinetic models applied to the experimental measurements, only the passing by the origin is that obtained thanks to Ginstling's model [7] presented in the equation (Eq. 3). This characteristic makes it possible to eliminate the surface and interface kinetic models.

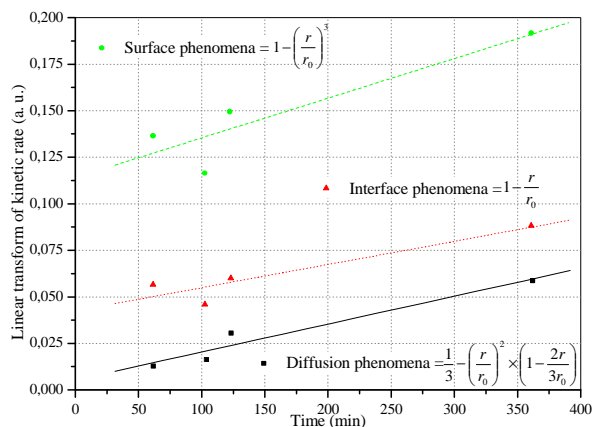


Figure 2: Linear transform of several kinetic models (diffusion, surface, interface) by Lindemer & al. [6]

However, even if they do not correspond to the phenomena observed, the graphic interpretations seem in all cases not very robust because of the lack of experimental data and of the poor obtained regression coefficients. By elimination, the diffusion model is thus only retained as being the determining reaction step. A post-mortem observation of the particles makes it possible to highlight two distinct reactional mechanisms according to the heat treatments.

The first configuration shows a UO_2 kernel surrounded by a UC_2 layer of uniform thickness. It was obtained after a fast heating to 1273 K in less than 2 minutes followed by 15 minutes temperature plateau (during which no carbide was still formed). Then, the sample is heated towards the final temperature according to a heating rate of 25°C/min and then cooled at - 50°C/min to prevent any risk of cracking of the particle.

The second configuration is obtained when the particles are submitted to important heating rates ranging between 50 and 100°C/min. These high heating rates induce the existence of strong thermal gradients inside a particle in spite of their small diameter (500 μm). The sample profiles have an non uniform aspect where UO_2 occupies the centre of the sphere and overflows partially towards external surface of the particle. This observation is not without pointing out the amoeba effect. This transfer phenomenon of carbon in gas phase is related to important heat gradients. The UO_2 kernel migrates towards the hot part of the particle. In some cases, caused displacement can be higher than the thickness of the external layer of the coated particle.

There is a noticeable difference between reaction rates of these two mechanisms. In the second case, the reaction rate of conversion is between two and five times faster than the first one. Logically, this difference in rate is attributed to a kinetic

control by different reactional steps. The comparison of the experimental results according to each protocol makes it possible Lindemer & al. to propose two distinct reactional mechanisms. The “uniform” kinetic scheme establishes the oxygen diffusion – starting from the interface between oxide and carbide through carbide and towards the surface of the particle – as the controlling step. On the contrary, in the case of the “non uniform” reaction, it is supposed that the $CO_{(g)}$ diffusion controls the kinetics.

The review of this study makes it possible to state that:

- the uranium carbide formation due to the reaction between UO_2 and C is controlled by the diffusion,
- the diffusion of $[O]_{UO_2}$ through UC_2 controls the kinetics when UC_2 encloses completely the UO_2 kernel,
- the reaction rate increases in the case of a “non uniform” reaction at the time of a fast increase of the sample temperature,
- the geometrical form and the physical contact of the reagents during conversion have a significant effect on the composition of the solid phase.

Nevertheless, these two mechanisms do not consider the interaction step between UO_{2+x} and carbon, during which, in a first step, uranium dioxide is reduced without carbide formation. It is thus also necessary to establish the behaviour of the interaction between UO_2 and carbon before the formation of a carbide phase.

Mukerjee's & al. studies [8] [9] deal with the carbothermic conversion of $UO_2 + C$ mixture to carbides under both vacuum and flowing argon. They are a good complement of Lindemer's & al studies. Indeed, in this case, the kinetics are both determined from $CO_{(g)}$ concentration measurements in a inert flowing gas and from manometric measurements under vacuum. Furthermore, the samples are mixed powders instead of coated particles. Thus, the experimental conditions are close to those used within our experimental measurements by High Temperature Mass Spectrometry (HTMS).

According to the experimental conditions, two distinct behaviours were highlighted: (i) under vacuum, the UO_2 reduction is controlled by reagent-product interface reactions whereas (ii) under a neutral gas flow, the $CO_{(g)}$ diffusion through the layer of carbide is the controlling step. Stinton & al. [10] postulated that during the carbothermic reaction performed on microspheres, surface nucleation is extremely fast and the particle is instantaneously covered by a thin carbide layer. In this case, the determining step becomes the propagation of the reactional interface towards the particle core controlled either by diffusion, by surface or by interface reactions.

Mukerjee's reaction route is based on Stinton's one [10] in which UC_2 dicarbide was substituted by UC monocarbide. The carbothermic steps are interface or diffusion reactions.

When the diffusion through the products layer is so fast that the reagents cannot sufficiently quickly combine with the interface reaction to establish equilibrium, the reaction rate is controlled by interface phenomena. By assuming that

nucleation occurs nearly instantaneously and that the reaction rate is proportional to the reagent surface not yet having reacted (S_t), the equation rate is written by the following way:

$$\frac{d\xi}{dt} = \frac{k \cdot S_t}{V_0} \quad (\text{Eq. 4})$$

After several operations [8], the previous equation can be put in a form highlighting the dependence of ξ with the initial radius of the particle (r_0):

$$1 - (1 - \xi)^{1/3} = \frac{k \cdot t}{r_0} \quad (\text{Eq. 5})$$

On the contrary, when the penetration of one of the reagents through the layer of products separating the two reactive phases is the determining stage, then the temporal dependence of the progressive accumulation of the product layer is inversely proportional to its thickness y .

$$\frac{dy}{dt} = \frac{k}{y} \quad (\text{Eq. 6})$$

After integration, this equation provides a parabolic equation which can be then written according to the ξ parameter. Jander [11] applied this equation to packed powders; it deduced the following law (Eq. 7) which is a function of a proportionality constant K and a diffusion coefficient D .

$$\left[1 - (1 - \xi)^{1/3}\right]^2 = \frac{2KDt}{r_0^2} \quad (\text{Eq. 7})$$

This last equation was modified by Zhuravlev, Lesokhin and Tempelman [12] by supposing that the activity of the reagent is proportional to the fraction not having reacted (Eq. 8). They obtain:

$$\left[\frac{1}{(1 - \xi)^{1/3}} - 1\right]^2 = \frac{2KDt}{r_0^2} \quad (\text{Eq. 8})$$

Valensi & Carter's model takes into account the difference between the product and the reagent densities consumed during the interaction. The assumption is made that the diffusion proceeds through layer of constant composition. After a valid first order approximation, the model appears as a simplified relation (Eq. 9):

$$\ln(1 - \xi) = \frac{kt}{r_0^2} \quad (\text{Eq. 9})$$

The degree of conversion of the reaction is established by measuring the quantity of $\text{CO}_{(g)}$ formed. Concerning the experiments under vacuum, measurement is only manometric. The realistic assumption is made that the gas composition is mainly made of $\text{CO}_{(g)}$. For the experiments performed under a gas flow, $\text{CO}_{(g)}$ formed is then oxidized into $\text{CO}_{2(g)}$ by passing through a copper catalyst. The quantities of $\text{CO}_{2(g)}$ are then evaluated by a titration of a NaOH solution.

The rate curves are characterized by a maximum of formation followed by a fall off of the reaction rate. At 1723 K, the rate becomes very slow for a value of ξ higher than 0.98. For lower temperatures, the reaction rate tends quickly towards a plateau.

Each kinetic model was used to treat these experimental data. For data under vacuum, the best curve is obtained by fitting the results with the equation that indicates that the UO_2/UC_2 interface reaction is the limiting step.

In the case of the experiments performed under gaseous flow, the reaction rate is much slower than in the case of those performed under vacuum and whatever the temperature, the reactional rate increases proportionally with the gaseous flow. The experimental data are interpreted thanks to Valensi & Carter's relation (Eq. 9), which indicates that in this case, the kinetics is controlled by diffusion phenomena.

Concerning the products analysis, one notes a larger quantity of dissolved oxygen in carbides formed at the lowest temperatures. This artefact phenomenon can be due to the low reaction rate which would confine the reagent under a layer of sintered carbide. At low temperatures, it is also possible that the main part of not reacted oxide disturbs the differentiation between the oxygen atoms forming oxide and those dissolved in carbides.

The later study of Mukerjee & al. [9] investigates the reactional mechanisms of the $\text{UO}_2 + \text{C}$ interaction using two types of samples. The first particle batch is made of $\text{UO}_2 + \text{C}$ mixed powders, as in the previous study. New microspheres were also synthesized, made up only of uranium dioxide dispersed in excess carbon black powder.

Under vacuum, the kinetic is much slower in case of the UO_2 microspheres dispersed in graphite than in the case of ($\text{UO}_2 + \text{C}$) microspheres. In this last case, the value of the C/UO_2 ratio has an effect on the composition of the products. For a ratio equal to 3, the formed carbide is UC and for a value of 4, the carbide is UC_2 . In case of an intermediate value, the products are a mixture of these two carbides. This result reveals the influence of the reagents proportions on the nature of the products related to the reaction trajectory inside the U-C-O system.

This new interpretation of the reactional mechanisms makes it possible to supplement the first Mukerjee's reactional mechanism [8] which only considered the UC carbide formation.

Like in his first study, the reaction kinetics is deduced according to interface phenomena. The interpretation confirms that the CO release is fast, which does not make it possible to clearly define the determining step among the proposed reaction mechanism:

1. $\text{C}_{(gr)} \rightarrow [\text{C}]_{\text{UC}}$
2. $\text{C}_{(gr)} \rightarrow [\text{C}]_{\text{UC}}$ diffusion from the surface towards the UO_2 -UC interface
3. $[\text{C}]_{\text{UC}} + \text{UO}_2 \rightarrow \text{UC} + 2 [\text{O}]_{\text{UC}}$
4. $[\text{O}]_{\text{UC}}$ diffusion towards the microsphere surface
5. $2 [\text{O}]_{\text{UC}} + 2 \text{C}_{(gr)} \rightarrow 2 \text{CO}_{(g)}$ at the surface

Two steps are likely to be the rate determining step: the diffusion of carbon or oxygen in the solid phase and through the product layer. The lack of carbide of higher degree during the intermediate steps of the $\text{UO}_2 + \text{C}$ conversion into UC lets suppose that a phenomenon of carbon diffusion could be the determining step when the experiments are performed under vacuum.

Contrary to the results obtained under vacuum, the kinetics of $\text{CO}_{(g)}$ formation under gas flow is controlled by the $\text{CO}_{(g)}$ diffusion through the layer of formed products. Moreover, the kinetics is dependent on the initial C/ UO_2 ratio of the samples. For a given temperature, time necessary for a complete reaction is longer as a function of the obtained products: UC_2 , $\text{UC} + \text{UC}_2$ and finally UC. To explain these different rates, a new mechanism is proposed including additional steps to the previous one:

6. $\text{CO}_{(g)}$ diffusion towards the UC_2 layer
7. $3 \text{UC}_2 + \text{UO}_2 \rightarrow 4 \text{UC} + 2 \text{CO}_{(g)}$
8. $[\text{C}]_{\text{UC}_2} \rightarrow [\text{C}]_{\text{UC}}$
Dissolution of C from UC_2 towards UC at the UC- UC_2 interface
9. Diffusion of $[\text{C}]_{\text{UC}}$ at the UC- UC_2 interface towards the UO_2 -UC interface
10. $[\text{C}]_{\text{UC}} + \text{UO}_2 \rightarrow \text{UC} + 2 [\text{O}]_{\text{UC}}$
Reaction between $[\text{C}]_{\text{UC}}$ and UO_2 at the UO_2 -UC interface
11. Diffusion of $[\text{O}]_{\text{UC}}$ formed at the UC- UO_2 interface towards the UC- UC_2 interface
12. $[\text{O}]_{\text{UC}} + \text{UC}_2 \rightarrow \text{UC} + \text{CO}_{(g)}$
Reaction between $[\text{O}]_{\text{UC}}$ and UC_2 at the UC- UC_2 interface

During this process, two interfaces must be considered: UC- UC_2 and UC_2 -($\text{UO}_2 + \text{C}$). The reactional steps involved at the UC_2 -($\text{UO}_2 + \text{C}$) interface are reactions 1. to 5., the step 6. corresponds to the $\text{CO}_{(g)}$ diffusion. In case of a total consumption of the free carbon at the external surface of the UC_2 layer, the interaction between trapped UO_2 and UC_2 proceeds according to the reaction 7.. It results the formation of a fine layer of UC between the UO_2 and UC_2 layers. The mechanism of interaction is described according to the steps 8. to 12.. The conversion of the $\text{UO}_2 + \text{C}$ microspheres into UC_2 proceeds according to a succession of steps during which the layer of dicarbide grows and generates a UC_2 microsphere. In this case, the reaction occurs according to steps 1. to 6.. The slower formation rate of UC could be due to the implication of reactions 7. to 12.. When conversion occurs according to reactions 1. to 12., the final size of the UO_2 core after the carbon disappearance determines the global reaction rate. The larger is the size of the UO_2 core, the slower are reactions 8. to 12..

Under vacuum, carbon diffusion is the limiting step of the carbide formation in $\text{UO}_2 + \text{C}$ microspheres. The assumed mechanism follows the same route as the previous one. But, since there is no intermediate product, the quantity of carbon available is sufficient to convert all the UO_2 into UC/ UC_2 without leaving core in the centre of the particle, the steps 7. to 12. should not occur.

EXPERIMENTAL STUDY

High Temperature Mass Spectrometry (HTMS), coupled with Knudsen effusion cells, is an high sensitivity experimental technique well adapted for performing partial pressures measurements [13-15]. In this method, the mean free path of the molecules in the molecular beam is such as it does not exist any shocks between the molecules during their sampling. A rarefied gas flow or molecular beam without collision goes through a diaphragm directly in the ionization chamber of a mass spectrometer maintained under high vacuum (Figure 3).

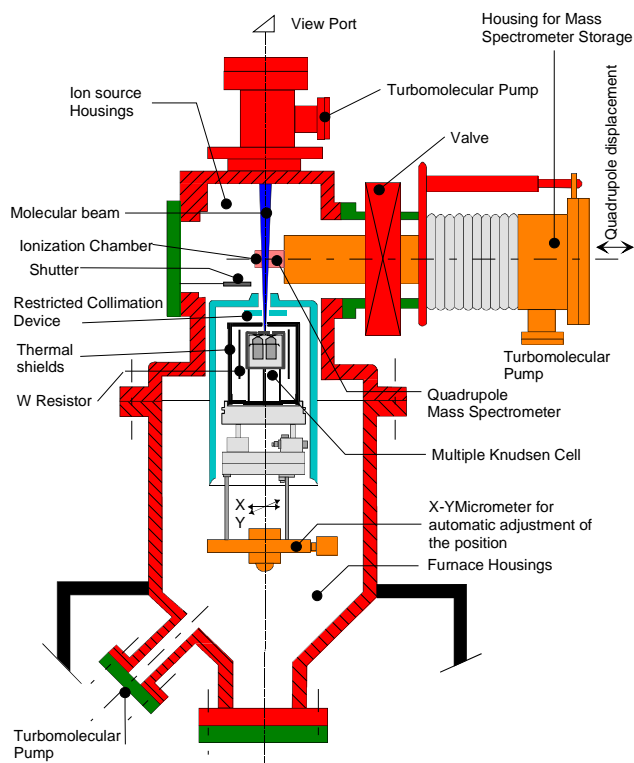


Figure 3: High Temperature Mass Spectrometer (HTMS) with multiple Knudsen cells

The gas ionization using an electron beam, will generate positive charged ions which are then extracted from the ionization chamber, accelerated by an electric field then separated according to their mass/charge ratio by a high frequency electric field. The Beer-Lambert law applied to the absorption of the electrons in a diluted medium leads to the basic mass spectrometric relation between the vapour pressures and the measured ionic intensities/temperature product:

$$p_i S_i = I_i T \quad (\text{Eq. 10})$$

The Knudsen effusion cells method is used much to analyze the gas phases at high temperature. The cell is a closed container; its lid is bored of a hole whose dimensions are small with respect to the surface of the sample. The flow of vaporized molecules from a surface s is the same one as the rarefied gas effusion flow resulting from a sufficiently large container (isotropy condition) by a same hole with ideally thin wall. The essential condition is that the mean free path of

the molecules in gas is higher than dimensions of the hole [1]. The flow of molecules in moles per unit of time which escapes from a hole of s surface is:

$$dn_i/dt \quad (\text{Eq. 11})$$

The total flow is obtained by integration on all the half space above the hole according to the Hertz-Knudsen relation [16]:

$$\frac{dn_i}{dt} = \frac{p_i s C}{\sqrt{2\pi M_i R T}} \quad (\text{Eq. 12})$$

In case of the $\text{UO}_2 + \text{C}$ interaction, the composition of the resulting gaseous phase is known [1]. In the U-C-O system, at least concerning the framework of TRISO fuel particles under nominal or accidental conditions, it is composed of a majority of $\text{CO}_{(g)}$ which can be sometimes supplemented by a few percents of $\text{CO}_{2(g)}$. $\text{CO}_{(g)}$ and $\text{CO}_{2(g)}$ ionic intensities measurements allow to determine the $\text{CO}_{(g)}$ and $\text{CO}_{2(g)}$ partial pressures, then the vapour phase composition. Measurements as a function of time allow to obtain the kinetics of formation of the gaseous phase. From the total mass loss during the experiment, the final overall composition of the sample can be determined in the U-C-O system. The phase compositions are measured from post-mortem analyse (SEM, XRD). These measurements do not require any additional calibration of the spectrometer since the mass loss (Δm) of the sample is known and is inevitably correlated with the gas products: $\text{CO}_{(g)}$ and $\text{CO}_{2(g)}$. Consequently, the loss of mass is used as internal standard.

For each gaseous species (i), it is possible to establish the molecular flow by associating the mass spectrometric and the Knudsen-Hertz relations (Eq. 10 & Eq. 12).

$$\frac{dn_i}{dt} = \frac{s C I_i T}{S_i \sqrt{2\pi M_i R T}} = \frac{s C I_i \sqrt{T}}{S_i \sqrt{2\pi M_i R}} \quad (\text{Eq. 13})$$

This equation highlights the proportionality between the molecular flow of a gaseous species and the product of the measured ionic intensities and the squared root of the temperature. For a defined geometry and a single vapour specie, all the others parameters can be considered as a single constant β_i . The integral of the last relation represents the amount of evaporated moles and so the loss of mass of the sample.

$$\beta_i = \frac{s \cdot C}{S_i \sqrt{2\pi M_i R}} \quad (\text{Eq. 14})$$

Then, the total amount of vaporized gas (in moles) can be evaluated by temporal integration of the molecular flow.

$$n_i(t) = \beta_i \int_0^t I_i \sqrt{T} dt \quad (\text{Eq. 15})$$

At the end of the experiment, the total amount of vaporized gas corresponds to the mass loss of the sample:

$$\beta_i = \frac{\Delta m}{M_{CO} \int_0^t I_i \sqrt{T} dt} \quad (\text{Eq. 16})$$

Then, the quantity of vaporized $\text{CO}_{(g)}$ moles according to time can be written as following:

$$n_{CO}(t) = \frac{\Delta m}{M_{CO}} \times \frac{\int_0^t I_{CO} \sqrt{T} dt}{\int_0^t I_{CO} \sqrt{T} dt} \quad (\text{Eq. 17})$$

In case of several gaseous species in the vapour composition (which is not considered here since the $\text{CO}_{2(g)}$ contribution is insignificant at high temperature), the specific mass spectrometer sensitivities (S_i) for each gaseous species (e.g. $\text{CO}_{(g)}$ and $\text{CO}_{2(g)}$) are established by an appropriate calibration of the mass spectrometer [14].

SAMPLES PREPARATION

The samples were manufactured from graphite and UO_{2+x} powders (with an initial O/U ratio of 2.06). Their respective molar proportions were 40% and 60%, that is to say roughly 2,5 g of UO_{2+x} and 0.075 g of carbon. After being mixed, these powders were packed and compacted under a manual press in a glove box in order to form compact pellets. The obtained green pellets are dense but in spite of the followed protocol, they remain friable and sometimes show cracks on their surfaces. The composition of the pellets, in particular the stoichiometry of uranium dioxide, has to be well controlled. Indeed, this parameter determines the oxygen potential in the ternary U-C-O system and influence strongly the kinetics of formation of the gaseous phase. Also, it determines the initial composition of the sample in the U-C-O system.

The stoichiometry measurement is performed on a UO_{2+x} green pellet taken from the same batch as the $\text{UO}_2 + \text{C}$ ones by Thermo-Gravimetric Analysis (TGA) according to an oxidation protocol of the dioxide UO_{2+x} into U_3O_8 . This cycle results from the literature critical analysis of the various calcination protocols of UO_{2+x} into U_3O_8 . Indeed, the main uncertainty on the evaluation of the composition of UO_{2+x} comes from the formation of under stoichiometric U_3O_8 at high temperature [17] [18]. The oxidizing gas flow is a Ar-20% O_2 mixture of argon and oxygen. The use of air is proscribed in order to avoid the formation of uranium oxynitrides which could alter measurement. By knowing the exact composition of the final oxidation product (stoichiometric U_3O_8) and by measuring the mass gain of the sample, the initial stoichiometry of UO_{2+x} is obtained. The test proceeds according to a heating rate of 10 K/min followed by a 35 minutes plateau at 1073 K during to UO_{2+x} oxidation. Then, the sample is cooled in order to stabilize the temperature to 873 K. This second plateau aims to fix exactly the stoichiometry of the oxide at the U_3O_8 composition. Indeed, for higher temperatures, the final product is under stoichiometric. A too fast decrease of the temperature, without passing by a final sufficiently long plateau at 873 K, would not let time to reach the equilibrium composition of U_3O_8 .

The stoichiometry of uranium dioxide which was initially equal to 2.06, has quickly evolved to a value of 2.15 and this in spite of the storage of the samples inside a glove box under nitrogen atmosphere.

RESULTS

The HTMS experiments were performed on $\text{UO}_{2+x} + \text{C}$ pellets of known initial composition and UO_{2+x} stoichiometry. The experimental approach consists in highlighting the formation of $\text{CO}_{(g)}$ and eventually $\text{CO}_{2(g)}$ and to quantify their partial pressure from ionic intensities measurements. Moreover, as indicated in the previous section, the composition of the sample can be deduced from the calculation of its mass loss.

The field of interest of formation of the gaseous phase is above 1273 K, approximate nominal temperature of VHTR reactors. Several experiments were performed in a range of temperature ranging between 1523 K and 1673 K, where the production of $\text{CO}_{(g)}$ starts to become significant. The analyzed gases are $\text{CO}_{(g)}$ and $\text{CO}_{2(g)}$. Measurements were also performed at the masses corresponding to the uranium gaseous species ($\text{UO}_{(g)}$, $\text{UO}_{2(g)}$, $\text{UO}_{3(g)}$); none of these species was detected.

The first experiments consisted in gradual heating of the samples in order to detect the temperatures from which $\text{CO}_{2(g)}$ and $\text{CO}_{(g)}$ begin to form, which are equal to respectively 1000 K and 1200 K. During these heat treatments, ionic intensity measurements appear in the form of gaseous puffs from which it is difficult to predict a kinetic behaviour. However, the ionic intensity curves confirm the preferential formation of $\text{CO}_{2(g)}$ (when it appears) (i) at low temperature and (ii) at the beginning of reaction. On the contrary, $\text{CO}_{(g)}$ is formed during the entirety of the experiment with a formation rate strongly related to the temperature. In all the cases, these experiments remain useful because they make it possible to follow the composition of the condensed phase. Moreover, the analyses of the samples by several methods (SEM, XRD) make it possible to know the formed products during this interaction. However, the most suitable method to determine kinetic behaviours is to perform heat treatments at a fixed temperature. So, after feasibility experiments, a simplified protocol was followed in order to facilitate the interpretation of the results.

The $\text{UO}_2 + \text{C}$ pellet was submitted to a fast heating rate to reach the plateau of 1603 K during 5 hours. The rise in temperature, from ambient towards the final temperature, was performed quickly and during this step, no signal appeared excepted a slight puff. This procedure was performed to avoid a low temperature $\text{CO}_{2(g)}$ production. So only the $\text{CO}_{(g)}$ ionic intensity was detected and measured (Figure 4).

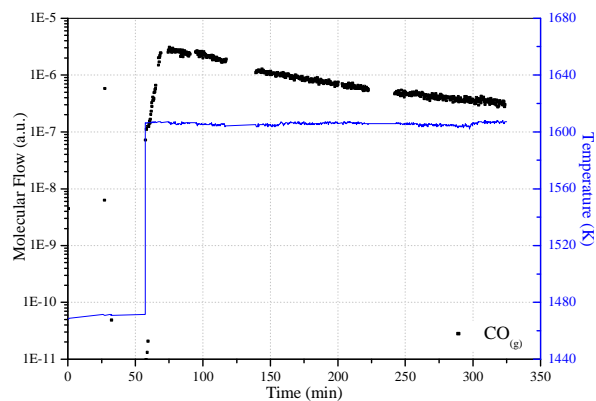


Figure 4: Measurement of the molecular flow of $\text{CO}_{(g)}$ vs time

The high temperature mass spectrometer was calibrated by the method of loss of mass of the sample [13] [14]. The obtained sensitivity of the mass spectrometer makes it possible to calculate the evolution of $\text{CO}_{(g)}$ pressure above the pellet (Figure 5). Thermodynamic calculations provide the stoichiometry of the uranium dioxide ($\text{O}/\text{U} = 1.998$) from which the first carbide phase appears during the UO_{2+x} reduction (Figure 5). From this value, the uranium dioxide cannot be more reduced and the carbon consumption is accompanied by the formation of carbide. This transition illustrates the composition path from the $\text{UO}_2 + \text{C}$ two-phase domain towards the $[\text{UO}_2 + \text{U}_2\text{C}_3 + \text{C}]$ three-phase domain (Figure 10). Thus, it becomes possible to compare it with the known equilibrium pressure of the $[\text{UO}_2 + \text{U}_2\text{C}_3 + \text{C}]$ three phase domain of the U-C-O system [1]. Moreover, this allows investigating the high temperature behaviour of the $\text{UO}_2 + \text{C}$ mixture and predicting if the interaction is preferentially governed by thermodynamics or kinetics phenomena.

Initially, the increase in pressure seems to be exponential until the delimitation between the two-phase and the three-phase domains which shows a maximum of pressure. Then, the pressure decreases slowly towards a plateau which is still not reached after 4 hours of heat treatment.

Two phenomena are then highlighted:

- Firstly, the shape of the curve of $\text{CO}_{(g)}$ pressure reveals that the time necessary to obtain a stationary regime seems long. To reach it, it would thus be necessary to lengthen the time of the experiment. However, this suggestion is synonymous with an additional consumption of $\text{CO}_{(g)}$ and thus of a displacement of the overall composition of the system U-C-O which would leave the $[\text{UO}_2 + \text{U}_2\text{C}_3 + \text{UC}]$ three-phase domain;
- Secondly, the pressure asymptote seems to tend towards pressure values largely lower than the thermodynamic equilibrium pressure (151.3 Pa). This behaviour highlights the role of the kinetics on the values of $\text{CO}_{(g)}$ pressure which are then different from the thermodynamic estimation concerning the $\text{UO}_2 + \text{C}$ interaction.

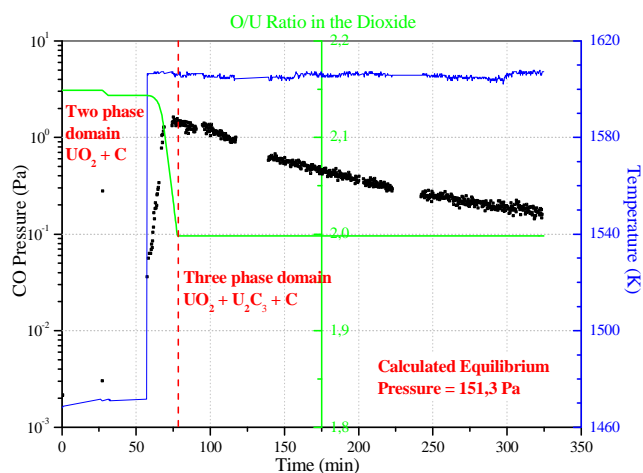


Figure 5: O/U Ratio in $\text{UO}_{2\pm x}$ and measurements of $\text{CO}_{(g)}$ pressure vs time compared to the equilibrium pressure (151,3 Pa) of the $[\text{UO}_2 + \text{U}_2\text{C}_3 + \text{C}]$ three phase domain

Experimental measurements of $\text{CO}_{(g)}$ pressure were processed according to the various models herein described (Zhuravlev, Mukerjee, Jander, Valensi & Carter). These relations were applied in order to describe the temporal evolution of the $\text{UO}_2 + \text{C}$ interaction represented by the loss of mass of the sample (Figure 7 – Figure 8). In parallel, temporal evolution of the degree of conversion ξ is also represented in order to compare the coherence of each model as a function of time.

Among the various models, the results seem to be more consistent with the relations (Eq. 5) and (Eq. 9), respectively corresponding to the models of Mukerjee and Valensi & Carter. In this last case, the linear regression applied to measurements is adjusted on a broad domain of degree of conversion of the reaction, from its start and up to 90%.

The currently available data do not allow settling between the various possible kinetic mechanisms because a wide range of temperature has to be investigated. However, the model suggested by Mukerjee seems more to be adapted to process the data. This statement is undoubtedly related to the similarities of our experimental conditions using High Temperature Mass Spectrometry and those reported by Mukerjee under high vacuum [8] [9].

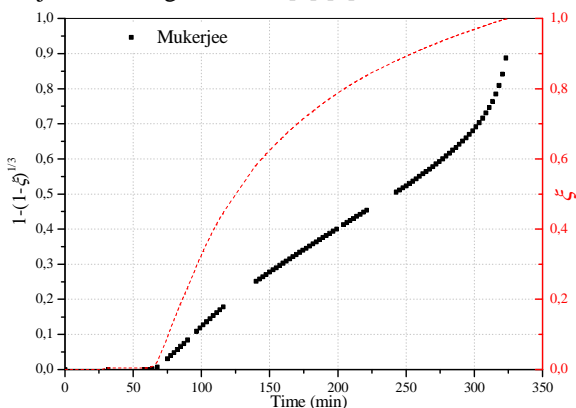


Figure 6: Processing of experimental measurements of $\text{CO}_{(g)}$ according to Mukerjee's model (Eq. 5)

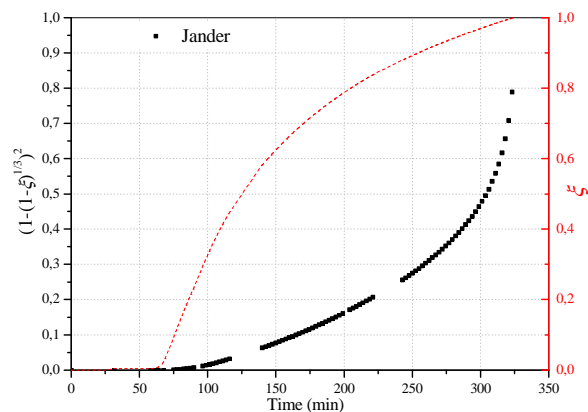


Figure 7: Processing of experimental measurements of $\text{CO}_{(g)}$ according to Jander's model (Eq. 7)

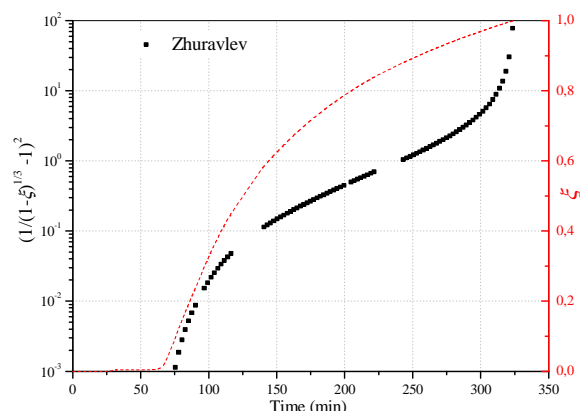


Figure 8: Processing of experimental measurements of $\text{CO}_{(g)}$ according to Zhuravlev's model (Eq. 8)

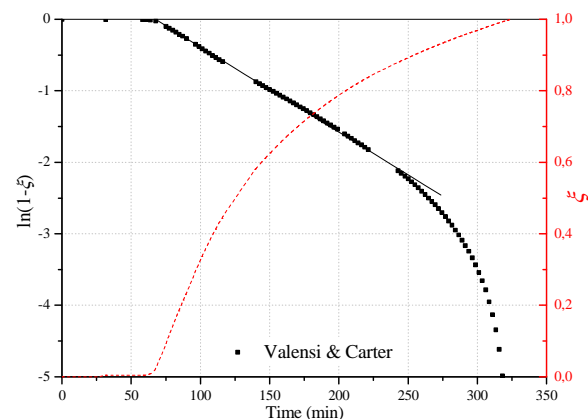


Figure 9: Processing of experimental measurements of $\text{CO}_{(g)}$ according to Valensi & Carter's model (Eq. 9)

Concerning $\text{CO}_{(g)}$, the treatment of the ionic intensity signal by the equations (Eq. 17) allows calculating the number of moles of $\text{CO}_{(g)}$ formed during the interaction. Thus, the variation of the overall composition of the sample can be represented inside the ternary U-C-O diagram calculated at the temperature of the experiment (Figure 10). The evolution of the $\text{UO}_2 + \text{C}$ interaction can be represented by a trajectory symbolizing the loss of gaseous species ($\text{CO}_{(g)}$ and/or of $\text{CO}_{2(g)}$). Thanks to this representation, it is possible to predict the phases normally expected by thermodynamics (Figure 10).

High Temperature Mass Spectrometry
CO Pressure Measurements (T=1606 K)

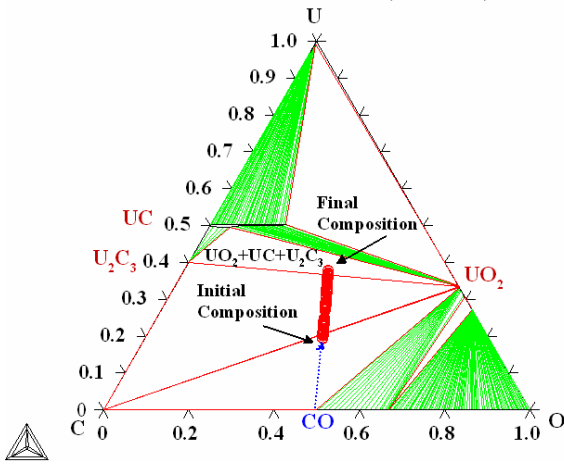


Figure 10 : Evolution of the total composition of the sample during the high temperature mass spectrometric experiment on a $UO_2 + C$ pellet

In this specific case, the final composition of the mixture is located inside the triangle corresponding to the three-phase domain equilibrium, formed of slightly under stoichiometric uranium dioxide UO_2 ($UO_{1.998}$), of uranium sesquicarbide U_2C_3 and of carbon C. After the experiment, the analysis of the samples by optical microscopy on polished section reveals an important proportion of a white phase located under the surface of the pellet (Figure 11).

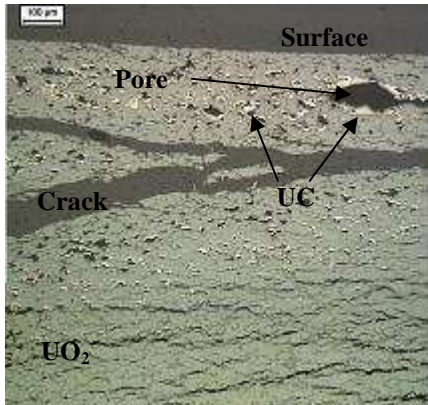


Figure 11: Optical microscopy on polished section of the pellet after heat treatment (Bulk = UO_2 , White phase = UC, Black hole = pores, Light gray = carbon)

This phase is mainly located inside the pores, which means that it is associated to the $CO(g)$ formation. Thus this phase corresponds to a carbide. On the contrary, the core of the pastille does not present this shining aspect any more which characteristic of the carbide phase. This observation suggests the presence of gradients of reactivity inside the pellet. So, it is possible that the UO_2 exists under different stoichiometries between surface and the core of the pellet in the range of composition from $UO_{1.998}$ to $UO_{2.15}$.

Furthermore, the X-Rays diffraction analysis of the pellet surface shows carbon and uranium carbide of the UC type associated to the white and brilliant phase. The analysis of the core of the same pellet after milling reveals no more carbon detectable and the proportion of UC seems more important in the bulk (Figure 12). This observation confirms the formation

of UC in the core of the pellet where the bulk is isolated by the carbide barrier in formation.

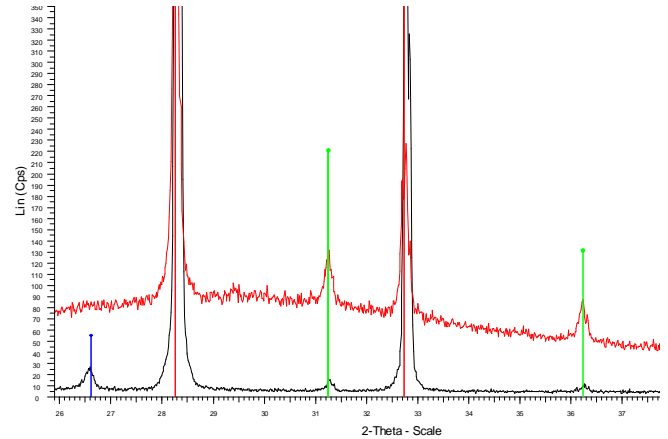


Figure 12 : X-Rays Diffraction Diagrams of the $UO_2 + C$ pellet (milled sample in red, surface in black) – In red: UO_2 , in blue C, green UC

CONCLUSION

This review of the main studies within the framework of the interaction between UO_2 and carbon highlights the various kinetic models available as well as the associated reactional mechanisms involved in this high temperature interaction.

HTMS experiments performed on the $UO_2 + C$ pellets confirm the strong interaction between these two compounds above 1000 K. As already mentioned [6], this interaction is characterized by the formation of a gaseous phase mainly constituted of $CO(g)$. The contribution of $CO_{2(g)}$ must be taken into account for a O/U ratio higher than 2, it decreases with the increasing temperatures. From the experimental point of view, $CO(g)$ is preferentially formed at the highest temperatures, $CO_{2(g)}$ is not formed any more above 1300 K.

The spectrometric results show the reduction of UO_{2+x} by the carbon which is symbolized by a rise in gas pressure. Then when the UO_2 reaches a limiting stoichiometry (O/U = 1.998), a carbide is formed and a three-phase domain is reached but without a pressure equilibrium being obtained, contrary to the thermodynamics calculations.

In addition, the measured pressures are very far from those calculated at equilibrium whereas the method of the Knudsen cell is usually employed to approach the conditions of a closed system at the equilibrium.

It was possible to apply various kinetic models to experimental measurements of $CO(g)$ formation by HTMS. Mukerjee's model [8] [9] fits the experimental results correctly. In this precise case, it seems that the reactional mechanism is governed by both interface and diffusion phenomena.

The observation of the samples confirms the formation of uranium carbide, UC or UC_2 in the case of experiment having exceeded the temperature of 1650 K. In this last case, as predicted by thermodynamics, the formation of the UC_2 carbide consolidates the idea according to which this compound is a high temperature phase. This statement is

corroborated by the most recent U-C assessed phase diagram [19].

Although the formation of sesquicarbure U_2C_3 is theoretically considered by thermodynamics, this compound was never identified by post-mortem analysis. Other experimental observations have already characterized this compound as "sluggish to be formed". These results show the importance of the kinetic limitations concerning the study of the $UO_2 + C$ interaction. These experiments show that the formed carbide is mainly localised on the edges of pores, of this fact it is consistent to associate it to $CO_{(g)}$ and/or $CO_{2(g)}$ gas release.

The difference between calculated pressures from thermodynamics and experimental values can be made profitable to evaluate evaporation coefficients. Their values will make it possible to establish the involved reactional limiting mechanisms: surface, interface or diffusion.

NOMENCLATURE

β = Integration constant
 C = Clausing coefficient
 Δm = Mass loss of the sample
 ξ = Degree of conversion
 I_i = Measured ionic intensity of the i species
 K, k = Reaction rate constant
 k_D = Diffusion rate constant (cm^2/s)
 m = Sample mass
 M_i = Molar mass of the i species
 p_i = Partial pressure of the i species
 r = UO_2 particle radius
 R = Perfect gas constant
 s = Surface
 S_i = Sensitivity of spectrometer for the i species
 t = Time ($0 = \text{initial}, f = \text{final}$)
 T = Temperature (K)
 V_0 = Initial volume of the fuel particle

ACKNOWLEDGMENTS

The authors thank EDF and Framatome-ANP for financial support of this study.

REFERENCES

- [1] Gossé S, Guéneau C., Chatain S., Chatillon C., 2006
Review of CO Pressure Measurements in the U-C-O Ternary System
Journal Nuclear Materials, In press
- [2] Guéneau C., Chatain S., Gossé S., Rado C., Rapaud O., Lechelle J., Dumas J. C., Chatillon C., 2005
A Thermodynamic Approach for Advanced Fuels of Gas Cooled Reactors
Journal Nuclear Materials, **344**, pp. 191-197
- [3] Petti D. A., Dolan T. J., Miller G. K., Moore R. L., Ougouag A. M., Oh C. H., Gougar H. D., 2002
Modular Pebble-Bed Reactor Project Laboratory-Directed Research and Development Program FY 2002 Annual Report

Idaho National Engineering and Environmental Laboratory,
EXT-02-01545

- [4] Danger G., Besson J., 1974
Etude Cinétique de la Carboréduction du Dioxyde d'Uranium
Journal of Nuclear Materials, **54**, pp. 190-198
- [5] Carter R. E., 1961
Kinetic Model for Solid-State Reactions
Journal of Chemical Physics, **34** (6), pp. 2010-2015
- [6] Lindemer T. B., Allen M. D., Leitnaker J. M., 1969
Kinetics of the Graphite-Uranium Dioxide Reaction from 1400°C to 1756°C
Journal of the American Ceramic Society, **52**, pp. 233-237
- [7] Ginstling A. M., Brounshtein B. I., 1950
Diffusion Kinetics of Reactions in Spherical Particles
J. Appl. Chem. USSR, **23** (12), pp. 1327-1338
- [8] Mukerjee S. K., Dehadraya J. V., Vaidya V. N., Sood D. D., 1990
Kinetic Study of the Carbothermic Synthesis of Uranium Monocarbide Microspheres
Journal of Nuclear Materials, **172**, pp. 37-46
- [9] Mukerjee S. K., Dehadraya J. V., Vaidya V. N., Sood D. D., 1994
Kinetics and Mechanism of $UO_2 + C$ Reaction for UC/UC₂ Preparation
Journal of Nuclear Materials, **210**, pp. 107-114
- [10] Stinton D. P., Tiegs S. M., Lackey W. J., Lindemer T. B., 1979
Rate-Controlling Factors in the Carbothermic Preparation of UO_2 -UC₂-C Microspheres
Journal of the American Ceramic Society, **62** (11), pp. 596-599
- [11] Jander W., 1927
Z. Anorg. Allg. Chem., **163** (01)
- [12] Zhuravlev V. F., Lesokhin I. G., Tempelman R. G., 1948
J. Appl. Chem. USSR, **21**, pp. 887
- [13] Chatillon C., 1998
La Spectrométrie de Masse à Haute Température : Données Accessibles et Développements Récents
La Revue de Métallurgie-CIT/Science et Génie des Matériaux, pp. 1077-1099
- [14] Heyrman M., 2004
Etude par Spectrométrie de Masse à Haute Température du Système Al_2O_3 -C : Application aux Fours d'Elaboration sous Vide
Ph. D. thesis supported at INPG, Grenoble – France
- [15] Baïchi M., Chatillon C., Guéneau C., Chatain S., 2001
Mass spectrometric study of UO_2 -ZrO₂ pseudo-binary system
Journal of Nuclear Materials, **294** (1-2), pp. 84-87
- [16] Carlson K. D., 1967
The Knudsen Effusion Method. The Characterization of High Temperature Vapors
Ed. J.L. Margrave, J. Wiley, New York, Chap. 5, pp. 115-129

- [17] Labroche D., Dugne O., Chatillon C., 2003
Thermodynamics of the O-U System. I: Oxygen Chemical
Potential Critical Assessment in the $\text{UO}_2\text{-U}_3\text{O}_8$ Composition
Range
Journal of Nuclear Materials, **312** (1), pp. 21-49
- [18] Guéneau C., Baïchi M., Labroche D., Chatillon C.,
Sundmann B., 2002
Thermodynamic Assessment of the Uranium-Oxygen System
Journal of Nuclear Materials, **304** (2-3), pp.161-175
- [19] Chevalier P. Y., Fischer E., 2001
Thermodynamic Modelling of the C-U and B-U Binary
Systems
Journal of Nuclear Materials, **288**, pp. 100-129

